Dissolution of Symmetric Diblock Copolymers with Neutral Solvents, a Selective Solvent, a Nonsolvent, and Mixtures of a Solvent and Nonsolvent Monitored by FT-IR Imaging

Beth A. Miller-Chou and Jack L. Koenig*

Department of Macromolecular Science, Case Western Reserve University, Cleveland, Ohio 44106

Received September 30, 2002; Revised Manuscript Received March 10, 2003

ABSTRACT: FT-IR imaging was used to study the dissolution of symmetric diblock copolymers of poly(styrene-*b*-methyl methacrylate) in neutral solvents (toluene and benzene), a selective solvent (2-ethoxyethanol), a nonsolvent (cyclohexane), and mixtures of the selective solvent and nonsolvent. 2-Ethoxyethanol is a good solvent for poly(methyl methacrylate) (PMMA) but a nonsolvent for polystyrene (PS), and cyclohexane is a nonsolvent for polystyrene below 35 °C and a nonsolvent for PMMA. Copolymer samples of three different molecular weights were tested with the neutral solvents, and one molecular weight was tested with the selective solvent, nonsolvent, and solvent mixtures. FT-IR images and concentration profiles were obtained, and dissolution rates were calculated from the concentration profiles. For the neutral solvent experiments, the block copolymer dissolution mechanism was governed by either solvent diffusion, which resulted in stress cracking for low molecular weights, or disentanglement of the polymer chains, which resulted in normal dissolution for higher molecular weights. The selective solvent dissolved the copolymer, and swollen, gel, and liquid layers were observed. The nonsolvent penetrated the bulk copolymer, but no dissolution occurred during the time of the experiments. Both the selective solvent and nonsolvent in the solvent mixtures penetrated the copolymer and produced similar results compared to the selective solvent or nonsolvent, depending on the weight fraction of each solvent in the mixture. The dissolution rate of the block copolymer was higher with mixtures of the selective solvent with the nonsolvent than for the neat selective solvent, but it decreased with increased weight percent of the nonsolvent.

Introduction

The dissolution of glassy polymers has been the subject of many studies for some time.[1−15] Polymer dissolution is an important aspect of many practical everyday applications and modern technologies such as time-release drugs[16,17] paint formation, membrane transport, and lithographic techniques used to manufacture microchips. The phase behavior of block copolymer solutions is also a subject of great interest.[18−24] Multicomponent nanoparticles' formation by self-assembly of different polymers and/or copolymers is a very topical problem, particularly for development of drug delivery systems, detergents, paints, cosmetics, and oil recovery.[22] Almost all applications of block copolymers involve mixtures, such as blends with a parent homopolymer, low molecular weight, "tackifying" resins and plasticizers, or solvents.[19] While there are several studies of the phase behavior, morphology, and micelle formation of block copolymers, there has been very little investigation and characterization of their dissolution mechanisms from the bulk state.

The dissolution process of any polymer can be influenced by the chemical structure, molecular weight of the polymer, thermodynamic compatibility of the solvent with the polymer, solvent size, and temperature. For a given block copolymer system, a solvent may be classified as neutral (a good solvent for both blocks) or selective (a good solvent for one block and a nonsolvent for the other). Therefore, the dissolution and phase behavior of block copolymers can vary greatly depending on the selectivity of the solvent, in addition to the symmetry of the block copolymer, chemical character of each block, and block length. Also, a neutral solvent should distribute itself equally between the two microdomains, whereas even a very slight degree of selectivity could lead to a measurable preferential swelling or segregation of one component.[23] However, for a solvent to be considered truly neutral, the two polymer−solvent interaction parameters (χ) would have to be exactly the same, which is unlikely. For example, Huang et al.[21] demonstrated a method, using small-angle neutron scattering (SANS), to quantify the small degree of selectivity that will generally exist for a block copolymer in a neutral solvent. In two diblock copolymers of poly(styrene-*b*-isoprene) with slightly different block lengths of polystyrene (PS), their analysis indicated that toluene was slightly selective toward polyisoprene (PI), and benzene and tetrahydrofuran (THF) were better solvents for PS. Selective solvents have also been studied in copolymer systems.[25,26] However, all these studies of block copolymers[18−26] have investigated the phase transitions and behavior of the polymer in the solution state and not the dissolution mechanism and rate. On the basis of these studies, however, variations of the block copolymers' dissolution mechanisms and rates are expected.

Two types/mechanisms of polymer dissolution have been established. With the first type of dissolution, termed "normal dissolution", all the layers described above are formed. The second type of dissolution occurs when no gel layer is observed. In a study by Asmussen and Raptis, poly(methyl methacrylate) (PMMA) was dissolved in several solvents and showed the normal dissolution process beginning at the glass transition temperature. By decreasing the experimental temperature, a steady decrease in the gel layer thickness could be seen until finally a temperature was reached where this part of the total surface layer was so thin that it

10.1021/ma0215363 CCC: $25.00
Published on Web 05/21/2003

was no longer visible. Below this temperature, cracks were observed running into the polymer matrix, and these cracks coalesced and caused small blocks of the polymer to leave the surface in a kind of eruption process. The reason for the cracking mechanism was proposed to be the freezing-in of large amounts of stress energy in the polymer in the glass transition interval. The gel temperature (where the transition from normal dissolution to cracking) was formally defined as the temperature at which the gel layer disappeared. Conversely with other experiments with polystyrene (PS), Ueberreiter and Asmussen observed that PS underwent normal dissolution in most solvents owing to its low gel temperature.

In this study, the dissolution of symmetric diblock copolymers of poly(styrene-*b*-methyl methacrylate) were monitored using FT-IR imaging. This technique has been used to study polymer dissolution[8,13,14,27] and provides simultaneous insight into both spatial and spectral data as a function of time of dissolution. Two neutral solvents, benzene and toluene, were used to dissolve each of the block copolymers of varying molecular weights, and the solvent penetration velocities were calculated. A selective solvent for PMMA, 2-ethoxyethanol, and a Θ solvent for PS ($T_\Theta = 35$ °C) and nonsolvent for PMMA, cyclohexane, were each used individually and as mixtures to dissolve one of the block copolymers. The goals of this study were (1) to utilize the FT-IR imaging technique to monitor the dissolution of block copolymers, (2) to monitor the dissolution process of a diblock copolymer made up of two polymers which normally dissolve by two very different mechanisms in the same solvent, (3) to determine whether either or both of the neutral solvents were selective toward one of the polymers, (4) to determine the effects of varying the solvent and copolymer molecular weight on the dissolution mechanism and rate, and (5) to establish a basis for further investigation of block copolymer dissolution using FT-IR imaging.

Experimental Section

Diblock copolymers of PS-*b*-PMMA with three molecular weights were purchased from Polymer Source, Inc.,[28] and used as received. The low molecular weight (LMW) copolymer had block lengths of $M_{nPS} = 5000$ and $M_{nPMMA} = 5000$; the medium molecular weight (MMW) copolymer had block lengths of $M_{nPS} = 12\,800$ and $M_{nPMMA} = 12\,900$; and the high molecular weight (HMW) copolymer had block lengths of $M_{nPS} = 50\,000$ and $M_{nPMMA} = 54\,000$. Benzene was purchased from Fisher Scientific,[29] and *d*-toluene, 2-ethoxyethanol, and *d*-cyclohexane (99.6% deuterated) were purchased from Aldrich Chemical Co.[30]

To prepare a thin layer of polymer sandwiched between two salt plates, a small amount of solid polymer was placed on a 2 mm thick CaF_2 substrate and was heated in an oven to 180 °C for 3 h (4 h for the HMW samples). Another substrate was then placed on top of the polymer, and a weight was applied on top of the substrate sandwich for 2 h. The weight was then removed, and the samples were allowed to cool in air to room temperature and stored in a desiccator until needed.

FT-IR imaging experiments were conducted using the contact method which has been described elsewhere.[31] At the time of the experiment, solvent was introduced from the empty end after the sampled interface was positioned in the spectrometer. The solvent entered the space between the substrates due to capillary action and came into contact with the polymer. Images were systematically acquired over time, and solvent was added as necessary so that the solvent remained in contact with the polymer at all times and the boundary condition was constant.

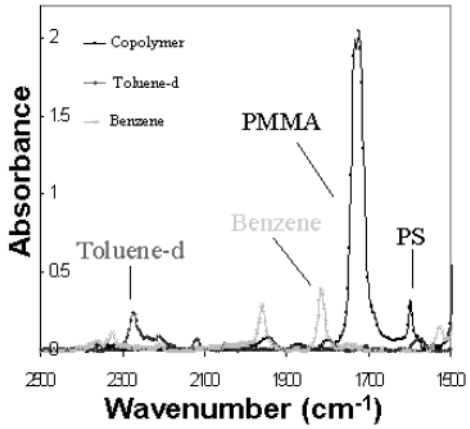

Figure 1. Absorbance spectra and characteristic peaks for the solvents and the block copolymer.

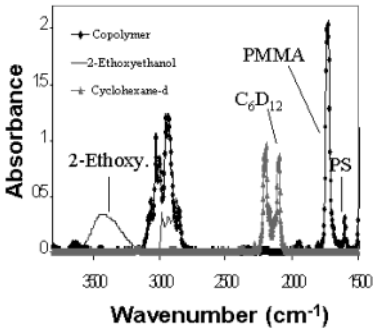

Figure 2. Absorbance spectra and characteristic peaks for the solvents and the block copolymer.

Infrared images were acquired using the Digilab Stingray[32] imaging spectrometer. The Stingray is comprised of an FTS 6000 step-scan interferometer bench coupled to a UMA-500 microscope accessory. The imaging detector is a Santa Barbara focal plane array of 64 × 64 mercury cadmium telluride (MCT) elements imaging an average spatial area of 400 μm × 400 μm in a single experiment. An 8 cm^{-1} nominal spectral resolution was used for the study. Image processing and data extraction were carried out using the hyperspectral imaging software packages Environment for Visualizing Images (ENVI)[33] and WinIR Pro.[32]

Each component of the system was monitored by a characteristic IR absorbance peak. Absorbance spectra for the neutral solvents and the copolymer can be seen in Figure 1. The peak at 1602 cm^{-1}, representing the ring quadrant stretching mode, was used to characterize the PS in the copolymer. The maximum peak at 1730 cm^{-1} (C═O stretch for the PMMA) could not be used for this study because of overabsorbance that causes problems with quantitative data analysis and calculations. Overabsorbance can be caused by the sample being too thick or the capacity to which a certain band will absorb is just very large. Generally, acceptable quantitative data can be interpreted from bands having an absorbance less than one. An experiment was performed where no overabsorbance occurred (a very thin sample) using the peak at 1730 cm^{-1}. The results using the points at 1755 and 1730 cm^{-1} for PMMA were compared, and they were found to produce the same qualitative and quantitative information. This method has been previously reported and validated.[34] Benzene was monitored by an overtone band at 1816 cm^{-1}, and deuterated toluene was monitored by the C−D stretch at 2121 cm^{-1}. Absorbance spectra for the selective solvent, nonsolvent, and the copolymer are shown in Figure 2. The 2-ethoxyethanol was monitored by the O−H stretch at 3457 cm^{-1}, and the peak at 2100 cm^{-1} (C−D stretch) was used to monitor the *d*-cyclohexane in the solvent mixtures. However, when neat *d*-cyclohexane was used, the peak at 2100 cm^{-1} overabsorbed and the

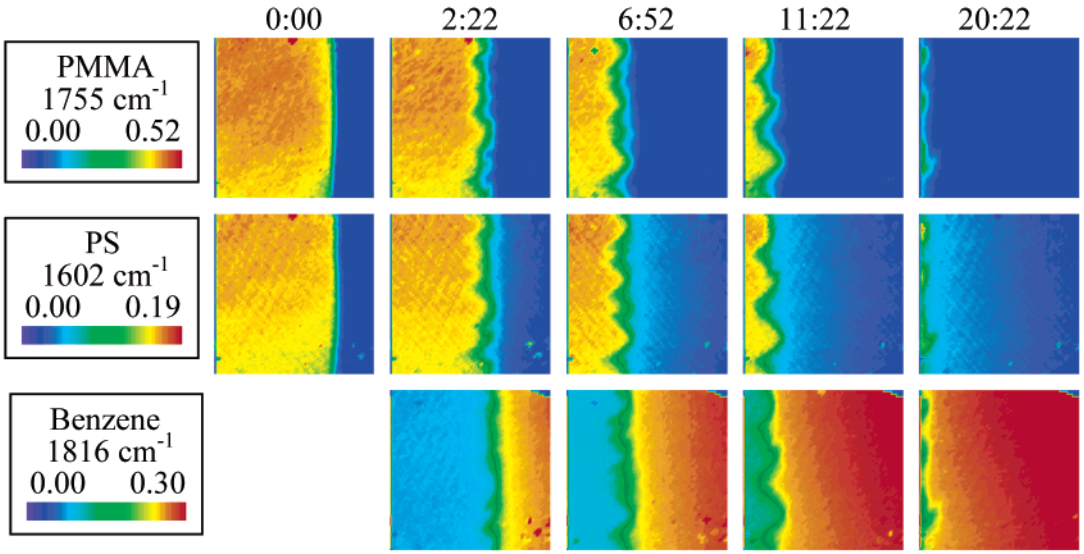

Figure 3. Images from the experiment of the dissolution of the LMW copolymer with benzene. The field of view is 400 μm × 400 μm, and the numbers on the top of each column represent the time of the experiment as minutes:seconds. The numbers above the color scale indicate the minimum and maximum absorbances of the peak/point imaged for each row.

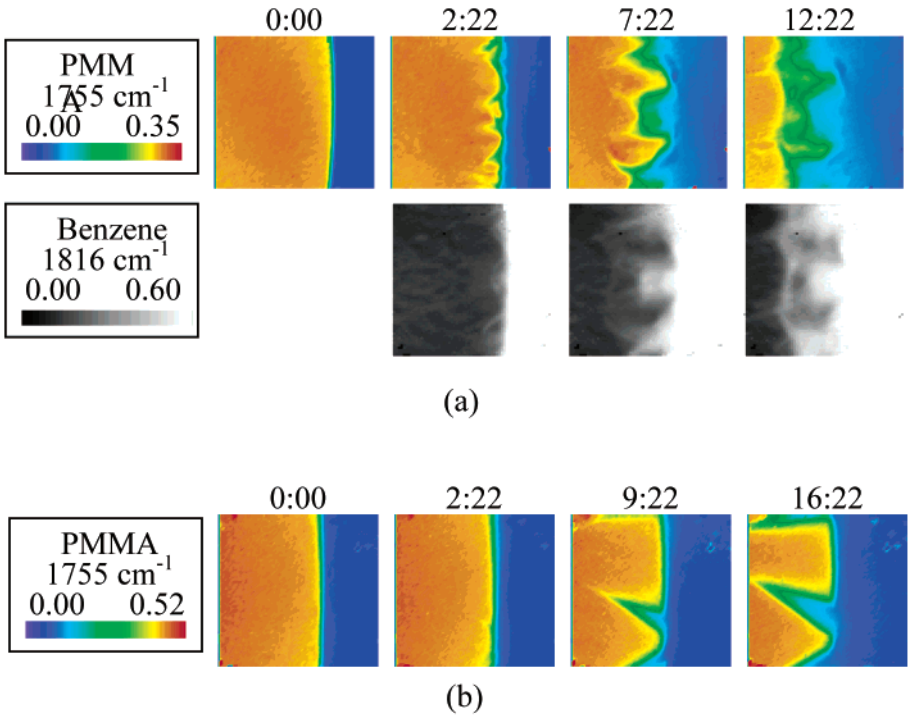

Figure 4. (a) PMMA and benzene images of the dissolution of the MMW block copolymer with benzene. (b) PMMA images of the dissolution of the MMW with toluene.

band at 2152 cm^{-1} had to be used instead. This band was tested and produced the same results as when the peak at 2100 cm^{-1} was monitored.

Results and Discussion

Copolymer Dissolution with Neutral Solvents. Each of the three different molecular weight block copolymers was tested with benzene and toluene, and both the dissolution mechanisms and rates were found to vary with molecular weight and solvent. Figure 3 shows the images from the experiment of the dissolution of the LMW copolymer with benzene. The images were obtained by plotting the characteristic absorbance frequency for each of the components. The images for the different components in the dissolution of the LMW copolymer with toluene were similar, and all the images were complementary when each of the components was plotted. However, the images for the MMW and HMW copolymers showed different results depending on the solvents. Parts a and b of Figure 4 represent the images of the dissolution of the MMW with benzene and toluene, respectively. The MMW copolymer showed a few large, sharp cracks with toluene and several small cracks with benzene, which are more evident in the black and white images in Figure 4a. The HMW copolymer also dissolved differently in the two solvents (Figure 5). With toluene the HMW copolymer developed a few large cracks, and no cracks appeared in the same copolymer with benzene. All experiments

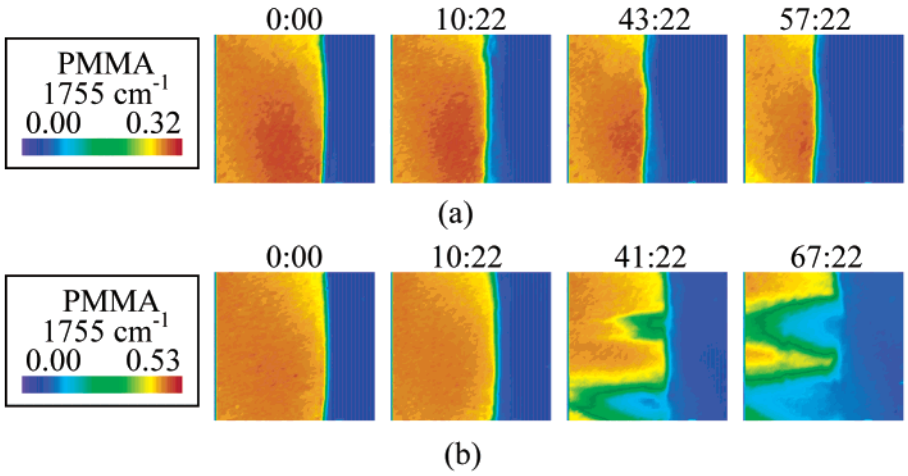

Figure 5. PMMA images of the dissolution of the HMW block copolymer with (a) benzene and (b) toluene.

were repeated with the same results. Therefore, it was concluded that the dissolution mechanism is dependent on both the molecular weight of the block copolymer and the solvent.

The copolymer entanglements play a key role in the dissolution process of the diblock copolymer. The entanglement molecular weights (M_e) for PMMA and PS are 7000 and 19 100 g/mol, respectively.[35,36] The LMW copolymer blocks are below the M_es for each of the polymers, and the same dissolution mechanism with both solvents was observed. However, some entanglements between the block copolymer chains exist, and we observe cracking, characterized by the development of a rough, uneven interface. In the MMW copolymer, the PMMA block molecular weights are higher than the M_e of PMMA while the PS block molecular weights are still below the M_e of PS. For this system, the block copolymer dissolves primarily by stress cracking. In the HMW copolymer, both the PMMA and PS blocks have molecular weights above their corresponding M_es, and the HMW block copolymer dissolves primarily by normal dissolution with benzene. Therefore, as the number of entanglements increased, the dissolution mechanism changed.

While PS and PMMA homopolymers have been known to dissolve with different mechanisms, further studies are needed to fully characterize the role that the copolymer composition plays in the dissolution mechanism. In this study, it has been concluded that the polymer entanglements are the primary factor in determining the dissolution mechanism of this block copolymer system. However, varied block lengths for a given total degree of polymerization of a high molecular weight copolymer could provide more insight into this topic.

With FT-IR imaging, absorbance profiles can be used to calculate the polymer dissolution rate. The dissolution rate can be determined by monitoring the position of the polymer−solvent interface as a function of time. The velocity of the interface can then be multiplied by the perpendicular area exposed to the solvent to obtain the dissolution rate. Since the perpendicular area remains constant, we can refer to the interface velocity as the dissolution rate, as it scales the same. The interface velocity was calculated by plotting the interface position vs time and obtaining the slope. If the copolymer dissolved with an uneven surface, as with the LMW copolymer systems and the MMW copolymer with benzene, three absorbance profiles were monitored at three positions of the images over time, and the corresponding three velocities were averaged to obtain the overall dissolution rate of the copolymer. If large cracks appeared in the copolymer sample, as with the MMW and HMW copolymers with toluene, the dissolution rate was monitored at a position on the interface where there were no cracks.

All plots had excellent linear fits except for the HMW copolymer with benzene (Figure 6). In this case, the plot has a changing slope at the beginning of the experiment indicating an induction time, which is characteristic of normal dissolution. This change in slope was not seen in the experiments where the copolymer dissolved via stress cracking, as dissolution by stress cracking characteristically does not show an induction time. There was also evidence of a gel layer, which can be seen in Figure 6b by the development of a second "hill" in the absorbance profiles with time. These data are consistent with our earlier conclusions that the block copolymer behaves as PS once the PS block lengths are higher than the M_e of PS, and normal dissolution occurs.

Solvent diffusion in glassy polymers is often characterized by a constant solvent penetration velocity (Figure 7a), which was observed with both benzene and toluene with all the block copolymers in our experiments. This non-Fickian behavior, termed case II diffusion,[37] is controlled by the polymer relaxation and is characterized by a sharp penetration front (Figure 7b) which advances at a constant rate. In the case of strong solvents, the gel layer can rapidly dissolve into the solvent and is typically not detectable. Thus, with strong solvents, case II diffusion gives rise to a constant dissolution rate.[38]

The dissolution rate for each solvent was plotted against total molecular weight of the block copolymer (Figure 8). Both systems (benzene and toluene) fit the polymer dissolution rate relation to molecular weight previously reported[15,39] as follows

$$s = kM^{-A} \tag{1}$$

where s is the solvent penetration rate, k is a constant which is dependent on temperature, M is the molecular weight, and A is a constant. For our systems, the dissolution rate with toluene was proportional to M_N^{-2}, and the dissolution rate with benzene was proportional to $M_N^{-0.1}$. The higher dissolution rates with benzene can

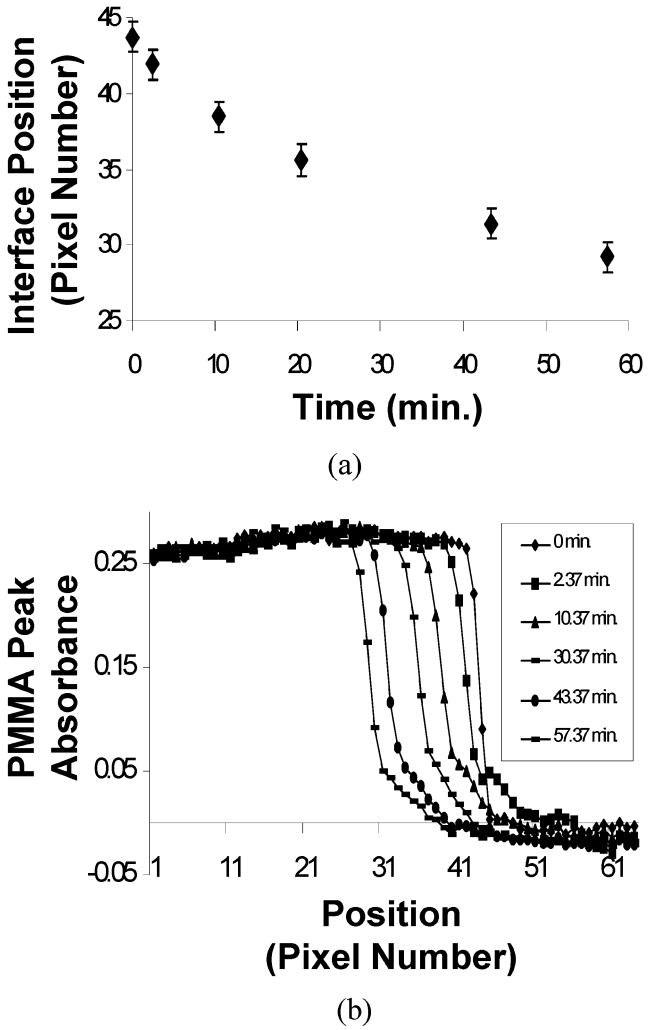

Figure 6. (a) Polymer−solvent interface position vs time and (b) PMMA absorbance profiles over time for the HMW copolymer dissolution in benzene.

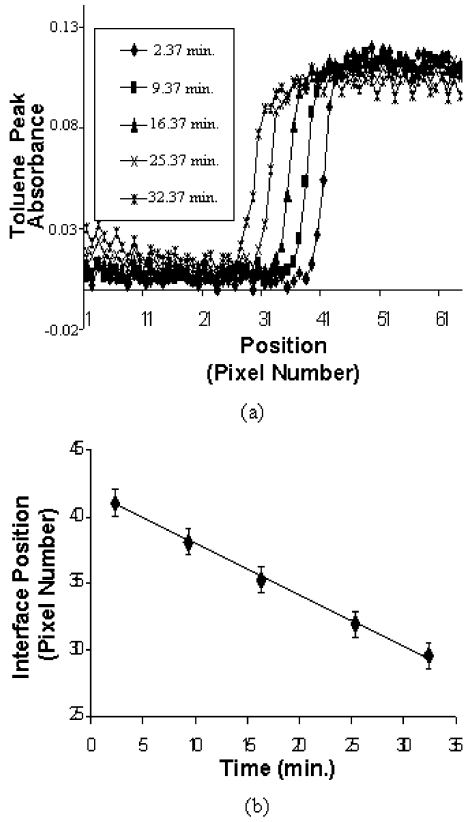

Figure 7. (a) Toluene absorbance profiles over time and (b) front position vs time for the MMW copolymer dissolution in toluene.

also be explained by the benzene's higher mobility (smaller size than toluene), a kinetic factor, and better thermodynamic compatibility with the copolymer.

This relation is similar to that incorporated into a polymer dissolution model developed Peppas et al.[25] where the dependence of the polymer dissolution rate on polymer molecular weight was derived showing that it was proportional to $M^{-\alpha/2}$. This model was developed by incorporation the polymer chain disentanglement mechanism into the relevant transport equations. The disentanglement time was used as a dissolution characteristic time controlling the moving position of the solvent−polymer boundary. It is important to note that Peppas's experimental studies of dissolution of PS and PMMA in MEK were used to verify the model, and two types of dissolution, normal and stress cracking, were observed. PS dissolved normally, and PMMA's dissolution was controlled by crack propagation. This same situation was observed with our systems when the block copolymer adopted the dissolution characteristics and mechanisms of one of the polymers composing the blocks. Therefore, our system fits very well with their model when the system is completely entangled and a gel layer develops, as was the case for polystyrene in their experiments.

The dissolution of a polymer in a solvent is known to involve two transport processes which are solvent diffusion and chain disentanglement. When an un-crosslinked amorphous glassy polymer is brought in contact with a thermodynamically compatible solvent, the latter diffuses into the polymer, and when the solvent concentration in the swollen polymer reaches a critical value, chain disentanglement begins to dominate and eventually the polymer dissolves.[40] This concept has been highlighted by dissolution models developed by Papanu et al.[41] and Narasimhan and Peppas.[40] In Papanu's model, the disentanglement rate (R_{dis}) of the polymer chain has the following relation with polymer molecular weight:

$$R_{dis} \sim M^{-2.5} \tag{2}$$

At low molecular weights, the polymer dissolution is controlled by the rate of solvent penetration, and at high molecular weights, it is controlled by the disentanglement rate. This is the mechanism for the system studied here. The solvents penetrate the copolymer slower than the chains can disentangle from the bulk copolymer with the LMW and MMW copolymers. However, once the block copolymer is completely entangled (both blocks are above their M_es), the solvents can penetrate faster than the chains can disentangle and a gel layer forms. The transition from diffusion-controlled to disentanglement-controlled dissolution occurs at a lower copolymer molecular weight for benzene since its penetration rate vs polymer molecular weight line is higher than that of the toluene (Figure 9).

It was also observed that the dissolution rates of the HMW copolymer were very similar for each of the solvents. This may imply that there is a critical molecular weight of the copolymer where the dissolution rate

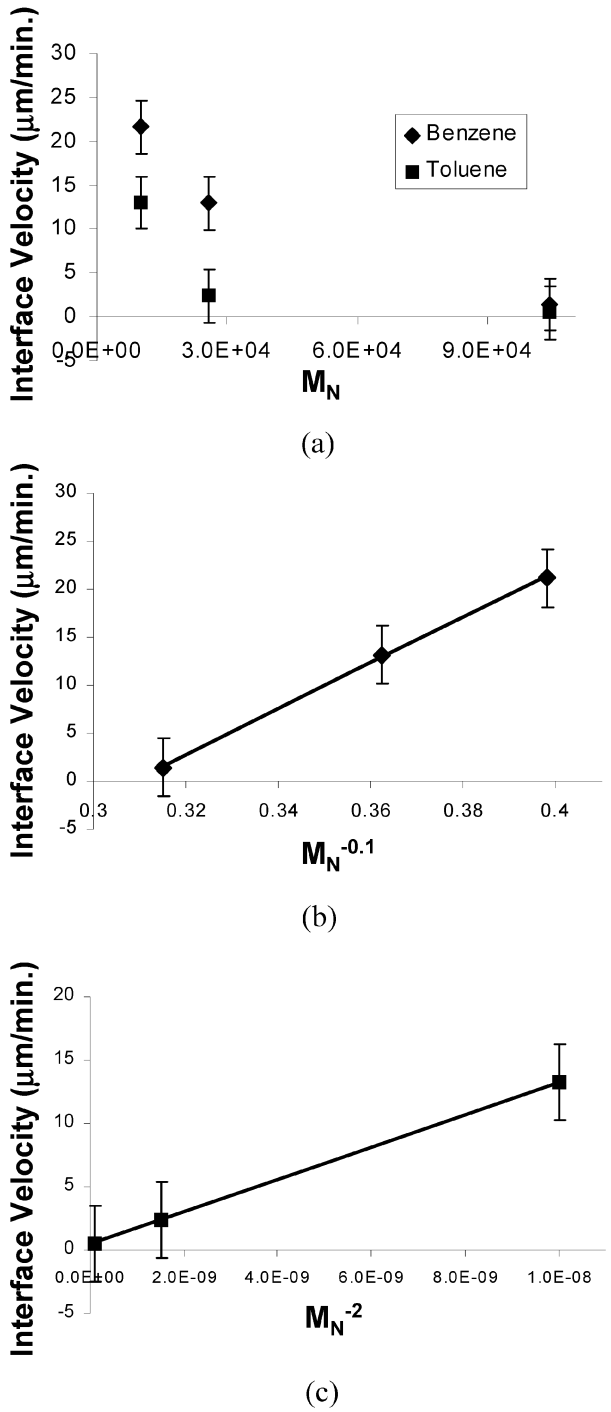

Figure 8. Polymer−solvent interface velocity vs (a) molecular weight of the block copolymer for both solvents, (b) $M_N^{-0.1}$ for dissolution with benzene, and (c) M_N^{-2} for dissolution with toluene.

becomes independent of the size of the penetrating solvent. Papanu et al.[42] observed that as the molecular weight of a polymer being dissolved was increased, the polymer film became more capable of supporting solvent-induced stress, and the solvent penetration rate decreased. At a sufficiently high molecular weight (10^5 g/mol) the film could readily support stress, and the solvent penetration rate became independent of molecular weight of the polymer. It is known that as the molecular weight of a polymer increases, the critical stress for crazing (and cracking), σ_c, increases since longer chains can support higher stress levels before the

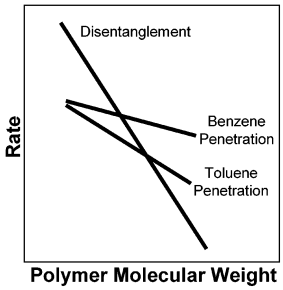

Figure 9. Schematic of rates vs polymer molecular weight. The lines are representative of the observed trends and are not based on actual calculated values.

onset of crazing. Specifically, the σ_c for PMMA has been found to increase with molecular weight until approximately 1×10^5 g/mol, after which it levels off to a constant value.[41] In our system, the dissolution rate does seem to level above 10^5 g/mol, but the dissolution rate also appears to become independent of the solvent used. This indicates that the dissolution is no longer controlled by the rate of solvent penetration, but it is controlled by the rate of disentanglement. On the basis of these results for our system, stress cracking is associated with diffusion-controlled dissolution and normal dissolution with a gel layer occurs when the controlling mechanism is the disentanglement rate.

The cracks in the sample dissolved with benzene are more numerous and appear earlier than the cracks that form with toluene. This phenomenon has been observed before by Miller-Chou and Koenig[8] and Ouano and Carothers.[9] This is due to the fact that benzene has a higher vapor pressure than toluene, is a thermodynamically better solvent for both PMMA and PS, and has a smaller size. As the solvents ingress into the polymer, pressure builds up because of the limited segmental mobility of the entangled chains. Eventually, the pressure gets high enough that fracture occurs and relieves the stress. Additional stresses are added to the system by the high vapor pressure of the benzene, which enhances the crack formation. In addition, the smaller size of benzene allows it to penetrate the polymer more efficiently and quickly than toluene.

Even though both benzene and toluene are good solvents for the copolymer, the benzene may be considered a better solvent since it dissolved each of the copolymers faster than toluene. This can be seen in the Flory−Huggins interaction parameter χ, which can be roughly estimated with the Hansen solubility parameters

$$\chi_{sp} = 0.34 + (V_r/RT)(\delta_s - \delta_p)^2 \qquad (3)$$

where the subscript sp indicates that we are considering the interaction between the polymer (p) and the solvent (s), V_r is the molar volume of the solvent, R is the gas constant, T is the temperature, δ_s is the solubility parameter of the solvent, and δ_p is the solubility parameter of the polymer.[43] χ is a dimensionless quantity for the thermodynamic description of polymer solutions. A lower χ value would indicate a lower free energy of mixing. The molar volumes and δ values were obtained from the literature,[44] and the χ_{sp} values were estimated for each of the polymer blocks with each of the solvents at room temperature. Since the solubility parameters of each of the solvents are very close, the primary difference in the χ values came from differences

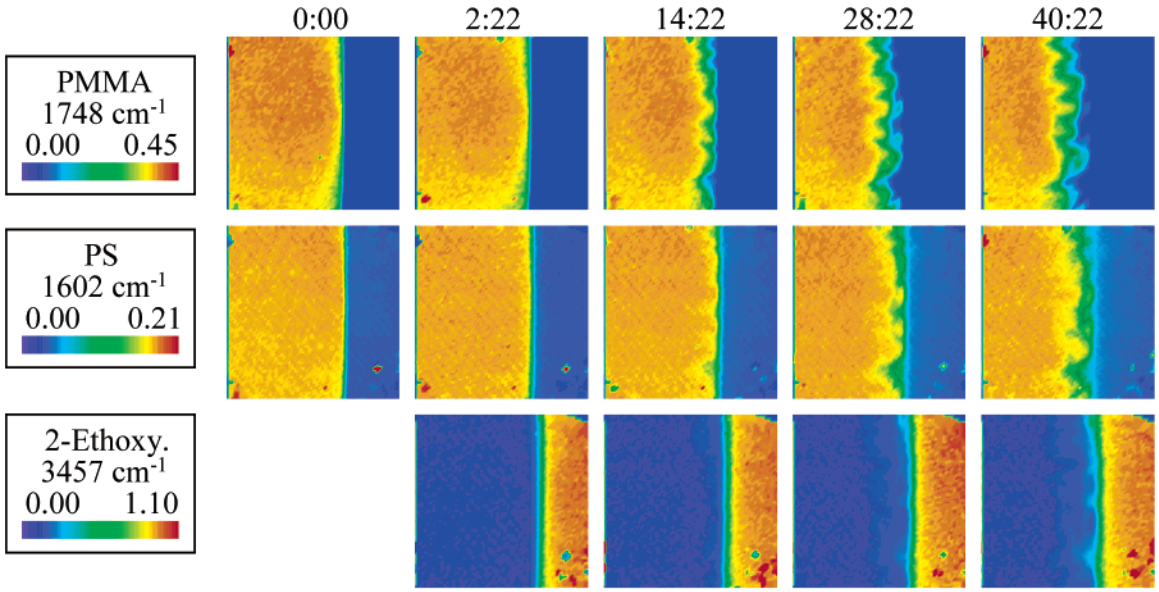

Figure 10. Images from the experiment of the dissolution of the copolymer with 2-ethoxyethanol.

in molar volume of the solvent, so the χ_{sp} values for benzene would be lower than those of toluene, and benzene may be considered a thermodynamically better solvent for the copolymer. In addition, the χ_{sp} values for both solvents would be lower for PS, compared with PMMA, which may indicate that they may be slightly selective toward PS. However, no apparent polymer segregation was observed in our experiments.

The issue of microphase separation can affect the dissolution process. It is understood that A-*b*-B diblock copolymer systems can undergo an order−disorder transition which results in a microphase separation transition (MST). This transition is controlled by the total degree of polymerization of the polymer chain, Z, the relative volume fractions of each block f_A or $f_B = 1 - f_A$, and the strength of the net A−B interactions generally modeled by the Flory−Huggins interaction parameter χ_{AB}. For a given pair of volume fractions, the MST occurs at a value of the product $\chi_{AB}Z$ which depends on f_A. For the case of our study, the f_A remains constant ($f_A \approx 0.5$), and the total degree of polymerization of the molecules is increased. The LMW copolymer is too short to be ordered, but the HMW copolymer is not. Since only one ordered state was tested, it is difficult to characterize the significance of the microdomains to the dissolution process and is beyond the scope of this paper. Further studies of high molecular weight copolymers with different block lengths and PS and PMMA domain sizes would be useful in characterizing the effects of these domains in combination with entanglement effects.

Block Copolymer Dissolution with a Selective Solvent. The LMW copolymer was tested with the selective solvent, nonsolvent, and solvent mixtures. This LMW copolymer was chosen so that the dissolution experiments could be completed in a reasonable experimental time. The dissolution behavior was completely different for the individual solvents, as expected from the previous observations discussed above. Figure 10 shows the images acquired when 2-ethoxyethanol was introduced to the block copolymer. The images were obtained by plotting the characteristic absorbance frequencies for each of the components. When the copolymer was exposed to 2-ethoxyethanol, the copolymer

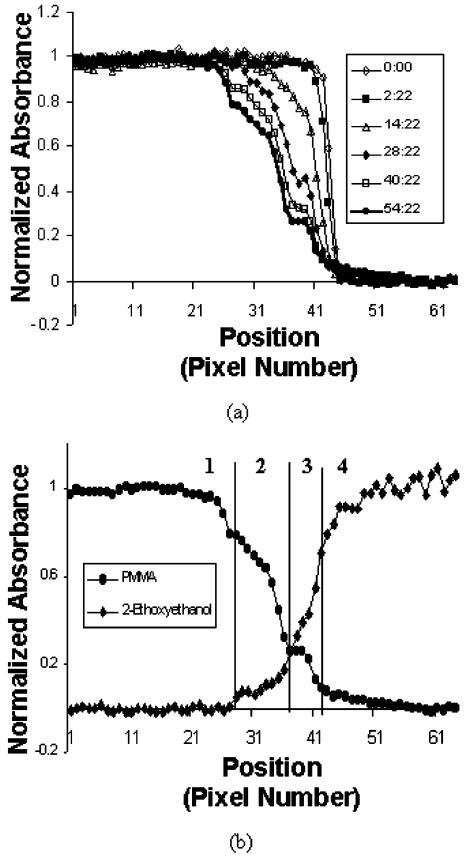

Figure 11. (a) PMMA absorbance profiles over time during the dissolution with 2-ethoxyethanol. (b) PMMA and 2-ethoxyethanol absorbance profiles after 54.37 min. Region 1 is the bulk copolymer, region 2 is the solid swollen layer, region 3 is the gel layer, and region 4 is the bulk solvent.

adopted the characteristics of both normal dissolution, as defined by Ueberreiter,[15] and stress cracking. Spatially separate layers developed over time and could easily be seen in the absorbance profiles (Figure 11). Region 1 represents the bulk copolymer, region 2 is the solid swollen layer, region 3 is the gel layer, and region 4 is the bulk solvent. Figure 12 is a plot of the interface

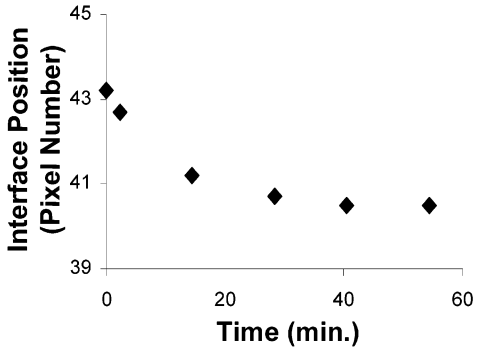

Figure 12. Bulk copolymer−solvent interface position vs time.

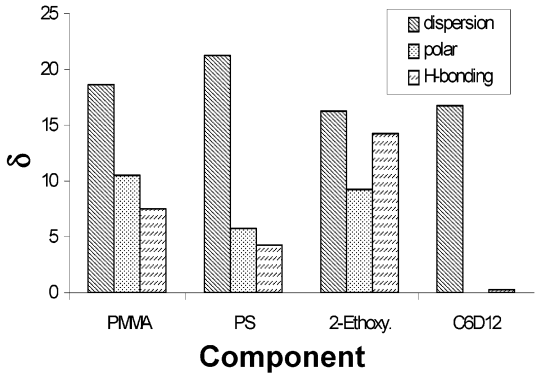

Figure 13. Hansen solubility parameters for PMMA, PS, 2-ethoxyethanol, and cyclohexane.

position vs time. Positions were labeled as pixel numbers, and the pixels increase from 1 to 64 from left to right across the image. One can see that the plot is nonlinear, and there is evidence of an induction time. The interface velocity decreases late in the experiment, and this is most likely due to an increase in the viscosity of the solvent due to the dissolved polymer chains within it; the solvent cannot penetrate the polymer as quickly since it has to travel through both the gel and swollen layers. In addition, the copolymer−solvent interface developed a rough edge over time, indicating stress cracking, and sharp cracks could be seen in the solvent images.

When the block copolymer was exposed to the neat nonsolvent, cyclohexane, no dissolution occurred over a period of 75 min, but the solvent did permeate the copolymer. This change in behavior, compared to the case of 2-ethoxyethanol, is related to the differences in the Hansen solubility parameters (Figure 13).[45] The cyclohexane has very low polar and hydrogen-bonding parameters compared with those of PMMA, PS, and 2-ethoxyethanol. 2-Ethoxyethanol has good thermodynamic compatibility which enables it to interact with the PMMA within the copolymer. However, the cyclohexane is not thermodynamically compatible with either of the polymer components, and even though the cyclohexane infiltrates the copolymer, the interaction of the main polymer PS chains with the cyclohexane molecules was less than the interaction of the main chains among themselves at a temperature below the θ temperature.[46]

Block Copolymer Dissolution with Solvent Mixtures. Experiments were conducted with solvent mixtures of the following 2-ethoxyethanol:*d*-cyclohexane initial weight ratios: 10:90, 20:80, 30:70, 40:60, 60:40, and 80:20. Mixtures with high 2-ethoxyethanol concentrations dissolved in the same fashion as with neat 2-ethoxyethanol and different dissolution layers could be distinguished. As the cyclohexane concentrations increased, the layers became less distinguishable, and at 70 wt % cyclohexane, none of the spatial layers were observed. However, dissolution still occurred at this weight ratio, which could be seen by the movement of the polymer−solvent interface over time, but the dissolution rate was very slow.

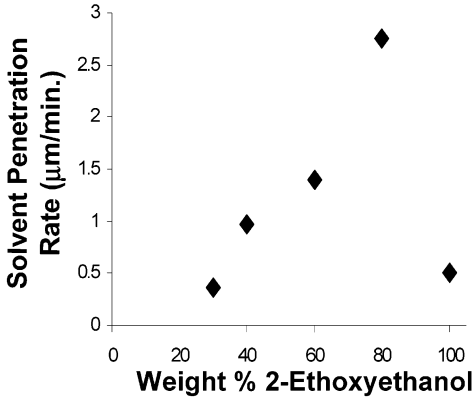

Figure 14. Solvent penetration rate vs wt % 2-ethoxyethanol in the solvent mixture with cyclohexane-*d*.

The solvent penetration rates were calculated from plots of the position of the inflection points of the solvents' absorbance profiles over time for experiments where significant dissolution occurred (mixtures with at least 30 wt % 2-ethoxyethanol). The rate was taken as the slope from the first three data points (up to 14 min of dissolution) before solvent penetration was slowed down by dissolved chains remaining at the polymer−solvent interface. Dissolved chains cause an increase in the viscosity of the solvent at the interface that acts to decrease further dissolution of the polymer. As the width of the dissolved polymer region increases with time, the dissolution process is hindered. The solvents penetrated the copolymer at the same rate, but the rate depended on the solvent mixture composition. As one can see in Figure 14, the solvent penetration rate of the mixtures was higher than the penetration rate of neat 2-ethoxyethanol. However, as the weight percent of 2-ethoxyethanol decreased within the mixture, the penetration rate also decreased. Therefore, a small amount of nonsolvent within the mixture enhances dissolution of the copolymer, which is a trend similar to previous studies with PMMA systems.[2,11,27,47]

A useful tool for predicting polymer dissolution is the solubility parameter, which was first developed by Hildebrand and Scott[48] with contributory work to this development by Scatchard and others.[49,50] Hildebrand defined the solubility parameter as

$$\delta = (E/V)^{1/2} \tag{4}$$

where E is the total cohesive energy and V is the molar volume of the pure solvent. E can be measured by evaporating the liquid of interest, i.e., breaking all the cohesive bonds.[51]

Today, a widely used approach to predicting polymer solubility is that proposed by Hansen.[52−54] The basis of the Hansen solubility parameters is that the total energy of vaporization of liquid consists of several individual parts which arise from atomic dispersion forces (D), molecular permanent dipole−permanent

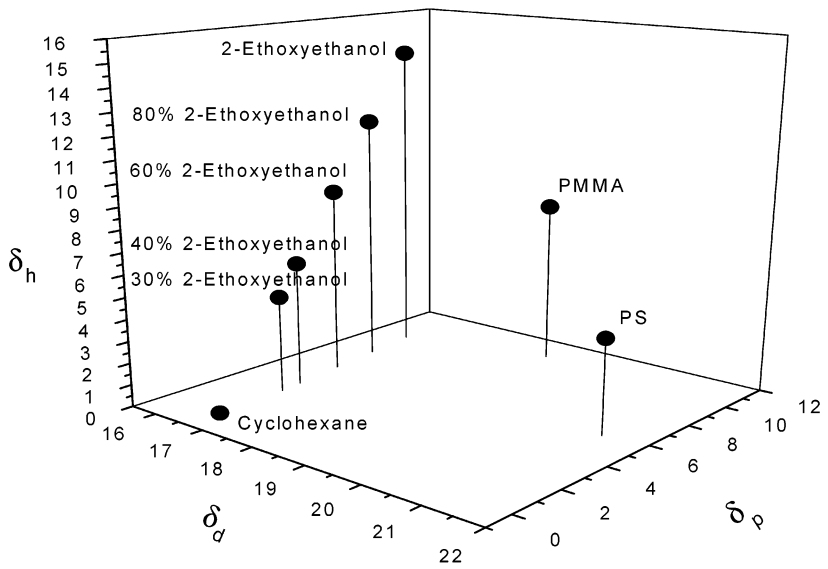

Figure 15. 3D graph of the Hansen solubility parameters (from the literature) for PMMA, PS 2-ethoxyethanol, cyclohexane, and the calculated solubility parameters of the solvent mixtures.

dipole forces (P), and molecular hydrogen bonding (electron exchange) (H).

$$\delta^2 = \delta_D{}^2 + \delta_P{}^2 + \delta_H{}^2 \quad (5)$$

Polymers will dissolve with solvents whose solubility parameters similar to that of the polymer.[51] Billmeyer suggests, as a good first approximation and in the absence of strong interactions such as hydrogen bonding, that solubility can be expected if $\delta_{polymer} - \delta_{solvent}$ is less than 3.5−4.0, but not if it is appreciably larger.[55] Hansen developed a characterization method using a solubility sphere.[51] With this method, the cohesion energy parameters of those liquids where affinities are highest are located within the sphere. The center of the sphere has the values of the δ_{DP}, δ_{PP}, and δ_{HP} parameters taken as being characteristic for the solute, the polymer in this case. A good solvent will have a solubility parameter positioned closer to that of the solute. Figure 15 is a 3D plot of the Hansen solubility parameters for the individual polymers within the block copolymer, solvents, and solvent mixtures. The solubility parameters of the mixtures were calculated as follows:

$$\delta_{H(AB\ mixture)} = \Phi_A\delta_{HA} + \Phi_B\delta_{HB} \quad (6)$$

$$\delta_{P(AB\ mixture)} = \Phi_A\delta_{PA} + \Phi_B\delta_{PB} \quad (7)$$

$$\delta_{D(AB\ mixture)} = \Phi_A\delta_{DA} + \Phi_B\delta_{DB} \quad (8)$$

where Φ is the volume fraction. The 80 and 60 wt % 2-ethoxyethanol mixtures' positions, as seen on the graph, are closer than 2-ethoxyethanol to that of the PMMA, indicating higher thermodynamic compatibility.

The magnitude of the radius of the sphere, Ro, is determined by the type of interaction being correlated. Skaarup developed the equation for the solubility parameter "distance", Ra, between two materials based on their respective partial solubility parameter components:

$$(Ra)^2 = 4(\delta_{DP} - \delta_{DS})^2 + (\delta_{PP} - \delta_{PS})^2 + (\delta_{HP} - \delta_{HS})^2 \quad (9)$$

Table 1

weight % 2-ethoxyethanol	Ra (with PMMA δs)
100	8.42
80	6.79
60	6.73
40	8.21
30	9.22

Therefore, good solvents have low Ra numbers and nonsolvents have high Ra numbers.

The Ra numbers for this study are listed in Table 1. Mixtures with 80%, 60%, and 40% 2-ethoxyethanol have lower Ra values and dissolve the copolymer faster than 100% 2-ethoxyethanol. However, once the 2-ethoxyethanol is at 30 wt %, the Ra value is larger than that of 2-ethoxyethanol, and the dissolution becomes slower than with neat 2-ethoxyethanol. Therefore, by observing the data on the 3D plot and the Ra values and correlating them with the dissolution rates, it is apparent that the mixtures with 40−80% 2-ethoxyethanol are thermodynamically better solvents for PMMA, and thus the dissolution of the block copolymer occurs more quickly for these mixtures.

According to a two-step model developed by Mao and Feng,[46] the dissolution of PS in cyclohexane can be explained as swelling below the Θ temperature and complete dissolution above the Θ temperature. Therefore, at 25 °C (temperature for our experiments) the cyclohexane only swells the polymer, and the side chain aromatic rings are gradually solvated by cyclohexane molecules. This process weakens the interactions between the phenyl rings themselves, thus allowing more motion of the phenyl groups. After the cyclohexane swells the polymer, the 2-ethoxyethanol can penetrate the copolymer more easily. This, in combination with an increase in thermodynamic compatibility, results in the dissolution occurring at a faster rate with these solvent mixtures.

Conclusions

FT-IR imaging has been successfully applied to examine the dissolution of a symmetric diblock copolymer, poly(styrene-*b*-methyl methacrylate), of varying molecular weights with two neutral solvents, benzene

and toluene. In addition, one of the copolymers was tested with a selective solvent, nonsolvent, and mixtures of the two.

With the neutral systems, the dissolution mechanism of the copolymer was governed by polymer entanglements, solvent activity, and solvent size. The dissolution mechanism changed from diffusion-controlled to disentanglement-controlled as the polymer molecular weight increased, which has been previously reported for homopolymers. This phenomenon is highlighted in polymer dissolution models previously developed.[40,41] The LMW block copolymer, which had block lengths smaller than the corresponding M_es of the PMMA and PS, dissolved the same with both solvents, but differences were seen at higher molecular weights. When the block length of the PMMA exceeded the M_e of PMMA, the copolymer took on PMMA characteristics and dissolved via stress cracking with no apparent induction time. However, when the block lengths of both PS and PMMA were larger than their corresponding M_es, the copolymer dissolved normally with an induction time and a smooth interface. For this system, stress cracking was associated with diffusion-controlled dissolution, and normal dissolution with a gel layer occurs when the controlling mechanism was the disentanglement rate of the polymer chains. The transition from one mechanism to the other occurs at different molecular weights depending on the solvent activity. Benzene was characterized as being more aggressive since it had a smaller χ_{sp} value and molar volume than toluene. This also explains higher dissolution rates when the copolymer was dissolved with benzene**.** Further investigation is needed to determine the extent to which the copolymer composition affects the dissolution process in combination with the effects of the entanglements and microphase separation.

The dissolution rates of each of the block copolymers were plotted against molecular weight of the block copolymer. Both systems (benzene and toluene) fit the polymer dissolution relation previously reported[15,39] and tested with homopolymers. For our system, the dissolution rate with toluene was proportional to M_n^{-2}, and the dissolution rate with benzene was proportional to $M_n^{-0.1}$. Case II solvent diffusion behavior was also observed.

When the copolymer was exposed to the selective solvent, 2-ethoxyethanol, the copolymer dissolved by a combination of stress cracking and normal dissolution, which could be characterized by the existence of an induction time and the presence of four different spatial layers: the bulk copolymer, the solid swollen layer, the gel layer, and the bulk solvent. When the block copolymer was exposed to the neat nonsolvent, cyclohexane, no dissolution occurred, but the solvent did infiltrate the copolymer. With mixtures of the solvents, the solvents penetrated the copolymer at the same rate, and the rate depended on the solvent mixture composition. The solvent penetration rate of some of the mixtures (down to 40 wt % 2-ethoxyethanol) was higher than the penetration rate of neat 2-ethoxyethanol, and it was concluded that a small amount of nonsolvent within the mixture enhanced dissolution of the copolymer. This enhancement was a combination due to swelling produced by the penetration of cyclohexane and improved thermodynamic compatibility between the polymer and solvent mixtures.

Acknowledgment. The authors acknowledge the financial support of the Polymer program of the Division of Materials Research under Contract DMR 0100428. The continued technical support of Digilab is also appreciated.

References and Notes

(1) Cooper, W. J.; Krasicky, P. D.; Rodriguez, F. *Polymer* **1985**, *26*, 1069−1072.
(2) Cooper, W. J.; Krasicky, P. D.; Rodriguez, F. *J. Appl. Polym. Sci.* **1986**, *31*, 65−73.
(3) Gipstein, E.; Ouano, A. C.; Johnson, D. E.; Need, O. U., III *Polym. Eng. Sci.* **1977**, *17*, 396−401.
(4) Krasicky, P. D.; Groele, R. J.; Rodriguez, F. *J. Appl. Polym. Sci.* **1988**, *35*, 641−651.
(5) Krasicky, P. D.; Groele, R. J.; Jubinsky, J. A.; Rodriguez, F. *Polym. Eng. Sci.* **1987**, *27*, 282−285.
(6) Manjkow, J.; Papanu, J. S.; Hess, D. W.; Soane (Soong), D. S.; Bell, A. T. *J. Electrochem. Soc.* **1987**, *134*, 2003−2007.
(7) Manjkow, J.; Papanu, J. S.; Soong, D. S.; Hess, S. W.; Bell, A. T. *J. Appl. Phys.* **1987**, *62*, 682−688.
(8) Miller-Chou, B. A.; Koenig, J. L. *Macromolecules* **2002**, *35*, 440−444.
(9) Ouano, A. C.; Carothers, F. A. *Polym. Eng. Sci.* **1980**, *20*, 160−166.
(10) Papanu, J. S.; Hess, D. W.; Bell, A. T.; Soane, D. S. *J. Electrochem. Soc.* **1989**, *136*, 1195−1200.
(11) Papanu, J. S.; Hess, D. W.; Bell, A. T.; Soane, D. S. *J. Electrochem. Soc.* **1989**, *136*, 3077−3083.
(12) Pethrick, R. A.; Rankin, K. E. *J. Mater. Chem.* **1998**, *8*, 2599−2603.
(13) Ribar, T.; Bhargava, R.; Koenig, J. L. *Macromolecules* **2000**, *33*, 8842−8849.
(14) Ribar, T.; Koenig, J. L. *Macromolecules* **2001**, *34*, 8340−8346.
(15) Ueberreiter, K. In *Diffusion in Polymers*; Crank, J., Park, G. S., Eds.; Academic Press: New York, 1968; p 219.
(16) Heller, J.; Baker, R. W.; Gale, R. M.; Rodin, J. O. *J. Appl. Polym. Sci.* **1978**, *22*, 1991−2009.
(17) Korsmeyer, R. W.; Lustig, S. R.; Peppas, N. A. *J. Polym. Sci., Part B: Polym. Phys.* **1986**, *24*, 395−408.
(18) Hanley, K. J.; Lodge, T. P. *J. Polym. Sci., Part B: Polym. Phys.* **1998**, *36*, 3101−3113.
(19) Hanley, K. J.; Lodge, T. P.; Huang, C.-I. *Macromolecules* **2000**, *33*, 5918−5931.
(20) Huang, C.-I.; Lodge, T. P. *Macromolecules* **1998**, *31*, 3556−3565.
(21) Huang, C.-I.; Chapman, B. R.; Lodge, T. P.; Balsara, N. P. *Macromolecules* **1998**, *31*, 9384−9386.
(22) Koňák, Č.; Helmstedt, M. *Macromolecules* **2001**, *34*, 6131−6133.
(23) Lodge, T. P.; Hamersky, M. W.; Hanley, K. J.; Huang, C.-I. *Macromolecules* **1997**, *30*, 6139−6149.
(24) Lodge, T. P.; Pudil, B.; Hanley, K. J. *Macromolecules* **2002**, *35*, 4707−4717.
(25) Tuzar, Z.; Kratochvil, P. In *Surface and Colloid Science*; Matijevic, E., Ed.; Plenum Press: New York, 1993; Vol. 15.
(26) Lodge, T. P.; Xu, X.; Ryu, C. Y.; Hamley, I. W.; Fairclough, J. P. A.; Ryan, A. J.; Pedersen, J. S. *Macromolecules* **1996**, *29*, 5955−5964.
(27) Gonzales-Benito, J.; Koenig, J. L. *Macromolecules* **2002**, *36*, 7361−7367.
(28) Polymer Source, Inc., Montreal, Quebec.
(29) Fisher Scientific, Pittsburgh, PA.
(30) Aldrich Chemical Co., Milwaukee, WI.
(31) Challa, S. R.; Wang, S.-Q.; Koenig, J. L. *Appl. Spectrosc.* **1996**, *50*, 1339−1344.
(32) Digilab Laboratories, Randolph, MA.
(33) Research Systems, Inc., Boulder, CO.
(34) Rafferty, D. W.; Koenig, J. L. *J. Controlled Release* **2002**, *83*, 29−39.
(35) Wunderlich, W. In *Polymer Handbook*, 4th ed.; Brandrup, J., Immergut, E. H., Grulke, E. A., Eds.; Wiley-Interscience: New York, 1999; Vol. 5, p 88.
(36) Shrader, D. In *Polymer Handbook*, 4th ed.; Brandrup, J., Immergut, E. H., Grulke, E. A., Eds.; Wiley-Interscience: New York, 1999; Vol. 5, p 92.
(37) Alfrey, T. A.; Gurnee, E. F.; Lloyd, W. G. *J. Polym. Sci., Part C: Polym. Symp.* **1966**, *12*, 249−261.

(38) Rodriguez, F.; Krasicky, P. D.; Groele, R. J. *Solid State Technol.* **1985**, *28*, 125−131.
(39) Asmussen, F.; Ueberreiter, K. *J. Polym. Sci.* **1962**, *57* 199−208.
(40) Narasimhan, B.; Peppas, N. *Macromolecules* **1996**, *29*, 3283−3291.
(41) Papanu, J. S.; Soane (Soong), D. S.; Bell, A. T.; Hess, D. W. *J. Appl. Polym. Sci.* **1989**, *38*, 859−885.
(42) Papanu, J. S.; Hess, D. W.; Soane (Soong), D. S.; Bell, A. T. *J. Appl. Polym. Sci.* **1990**, *39*, 803−823.
(43) Painter, P.; Coleman, M. *Fundamentals of Polymer Science*, 2nd ed.; Technomic Publishing Co., Inc.: Lancaster, 1997; p 318.
(44) Grulke, E. A. In *Polymer Handbook*, 3rd ed.; Brandrup, J., Immergut, E. H., Grulke, E. A., Eds.; Wiley-Interscience: New York, 1989; Vol. 2, p 675.
(45) Grulke, E. A. Solutiblity Parameter Values. In *Polymer Handbook*, 3rd ed.; Brandrup, J., Immergut, E. H., Grulke, E. A., Eds.; Wiley: New York, 1989; Vol. II, p 675.
(46) Mao, S.-Z.; Feng, H.-Q. *Colloid Polym. Sci.* **1998**, *276*, 247−251.
(47) Miller-Chou, B. A.; Koenig, J. L., submitted to *J. Polym. Sci., Part B: Polym. Phys.*
(48) Hildebrand, J. H.; Scott, R. L. *The Solubility of Nonelectrolytes*, 3rd ed.; Dover Publications: New York, 1964.
(49) Scatchard, G. *Chem. Rev.* **1931**, *8*, 321−333.
(50) Scatchard, G. *Chem. Rev.* **1949**, *44*, 7−35.
(51) Hansen, C. M. *Hanson Solubility Parameters: A User's Handbook*; CRC Press: Boca Raton, FL, 2000.
(52) Hansen, C. M. *J. Paint Technol.* **1967**, *39*, 104−117.
(53) Hansen, C. M. *J. Paint Technol.* **1967**, *39*, 505−510.
(54) Hansen, C. M.; Skaarup, K. *J. Paint Technol.* **1967**, *39*, 512−514.
(55) Billmeyer, F., Jr. *Textbook of Polymer Science*; Wiley-Interscience: New York, 1984.

MA0215363